Electronic Supplementary Information

Interface Passivation with $Ti_3C_2T_x$-MXene Doped PMMA Film for Highly Efficient and Stable Inverted Perovskite Solar Cells

João Pedro F. Assunção[a]; Hugo G. Lemos[a*]; Jessica H. H. Rossato[a]; Gabriel L. Nogueira[a]; João V. M Lima[a]; Silvia L. Fernandes[b]; Rafael K. Nishihora[c], Ricardo V. Fernandes[d], Sidney A. Lourençoe, Diego Bagnis[b], Sydney F. Santos[c], Carlos F. O. Graeff[a*]

[a] *São Paulo State University (UNESP), School of Sciences, Department of Physics, Bauru, SP, 17033-360, Brazil*

[b] *Oninn - Innovation Center, Belo Horizonte, MG, 31035-536, Brazil*

[c] *Federal University of ABC (UFABC), Center for Engineering, Modeling and Applied Social Science, Santo André, SP, 09210-580, Brazil*

[d] *Materials Science and Engineering Program (PPGCEM), Federal Technological University of Paraná (UTFPR), Londrina, PR, Brazil*

* *Corresponding author:* hugo.lemos@unesp.br; carlos.graeff@unesp.br

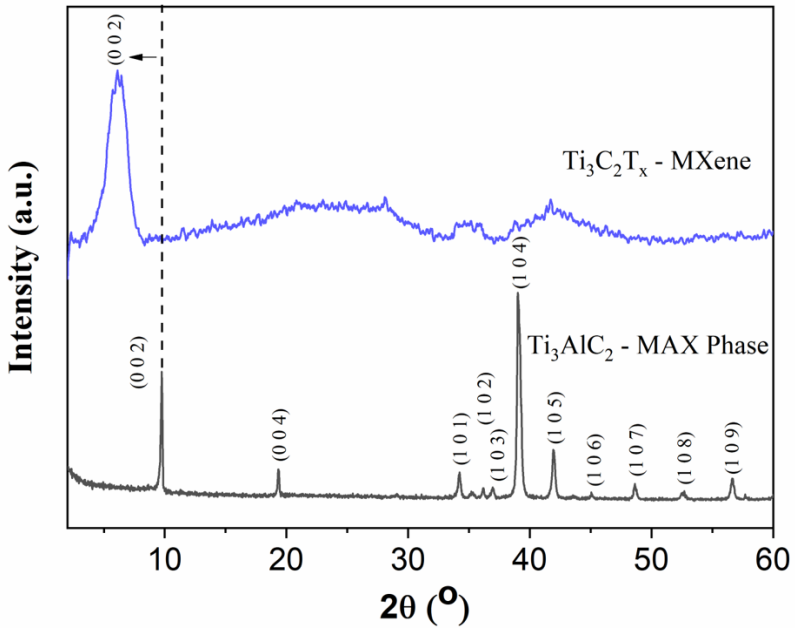

Figure S1: XRD patterns of Ti_3AlC_2 MAX phase and $Ti_3C_2T_x$ MXene.

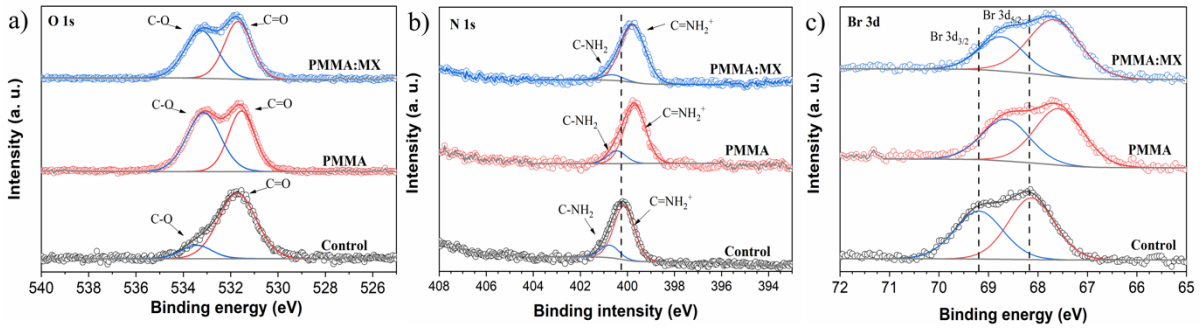

Figure S2: High-resolution XPS spectra of (a) O 1s, (b) N 1s and (c) Br 3d from bare perovskite, and perovskite containing PMMA and PMMA:MX-3% passivation layers.

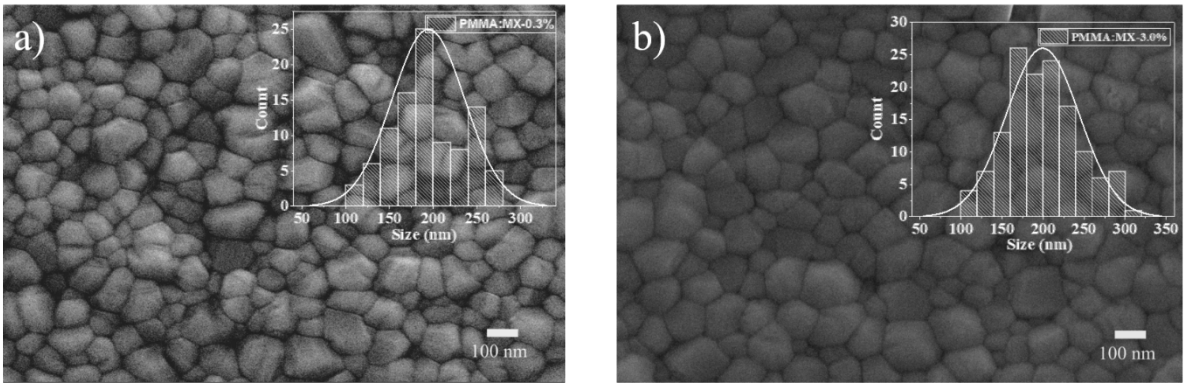

Figure S3: Grain size distribution measurements of perovskite containing (a) PMMA:MX-0.3% and (b) PMMA:MX-3% passivation layers.

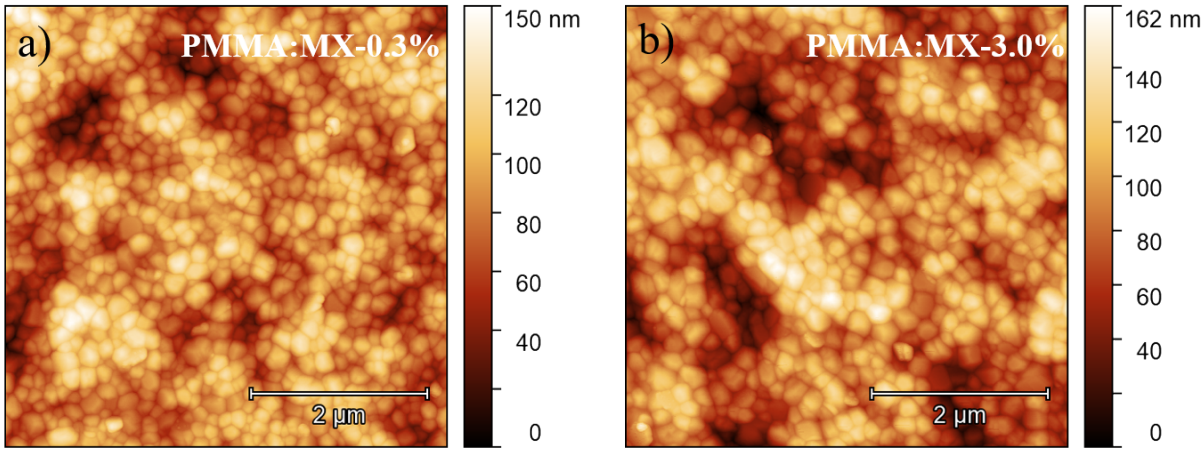

Figure S4: AFM images of perovskite containing (a) PMMA:MX-0.3% and (b) PMMA:MX-3.0% passivation layers.

Table S1: Contact angle (CA) measurements of bare perovskite, PMMA and PMMA:MX films to the ETL precursor solution (PCBM in CB).

Sample	Left angle (°)	Right angle (°)	Average angle (°)
Bare	43.06	17.56	30.31
PMMA	11.82	13.06	12.44
PMMA:MX-0.3%	13.53	11.22	12.37
PMMA:MX-1.5%	11.89	11.15	11.52
PMMA:MX-3.0%	10.78	17.23	14.01

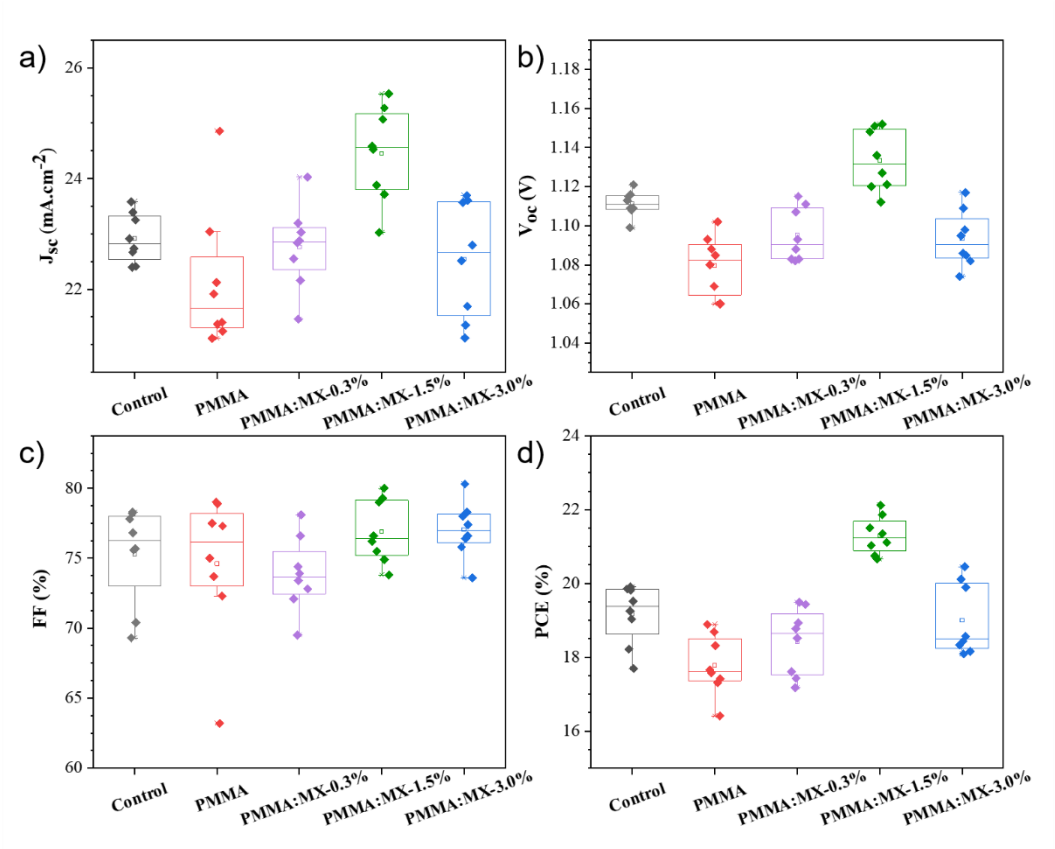

Figure S5: Box plots of the parameters (a) J_{SC} (mA.cm^{-2}), (b) V_{OC} (V), (c) FF (%) and (d) PCE (%) of PSCs.

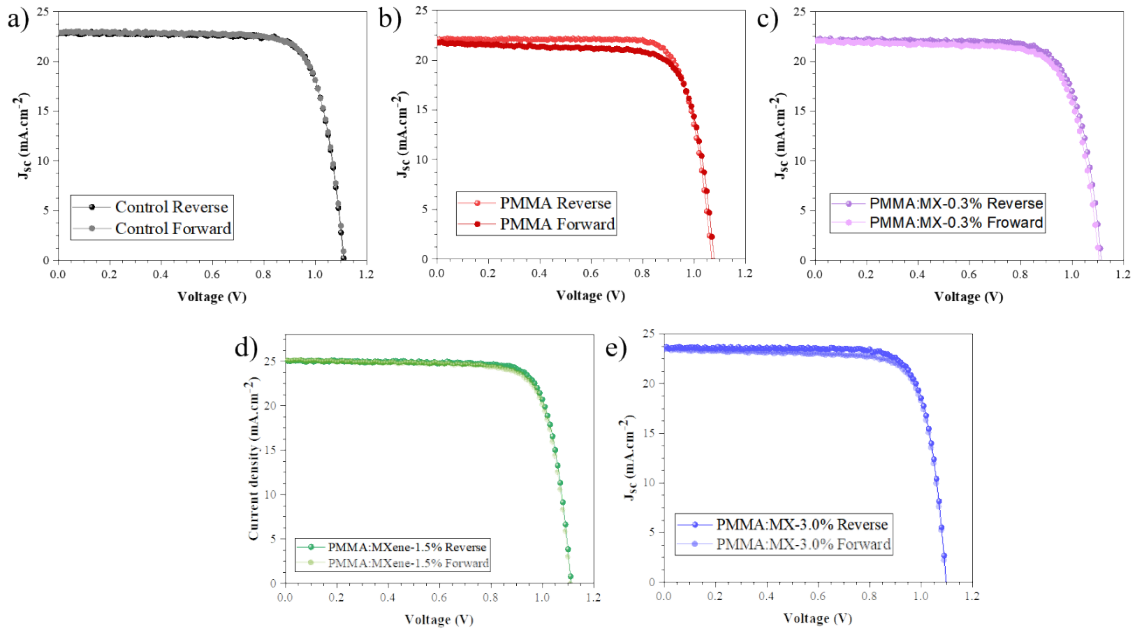

Figure S6: J-V curves of the best PSCs (a) Control, (b) PMMA and (c-e) PMMA:MX (0.3, 1.5 and 3%) respectively, for both reverse and forward directions.

The hysteresis index (HI) calculations were carried out using the following equation:

$$HI = \frac{PCE_{rev} - PCE_{for}}{PCE_{rev}} \qquad \text{(Eq. S1)}$$

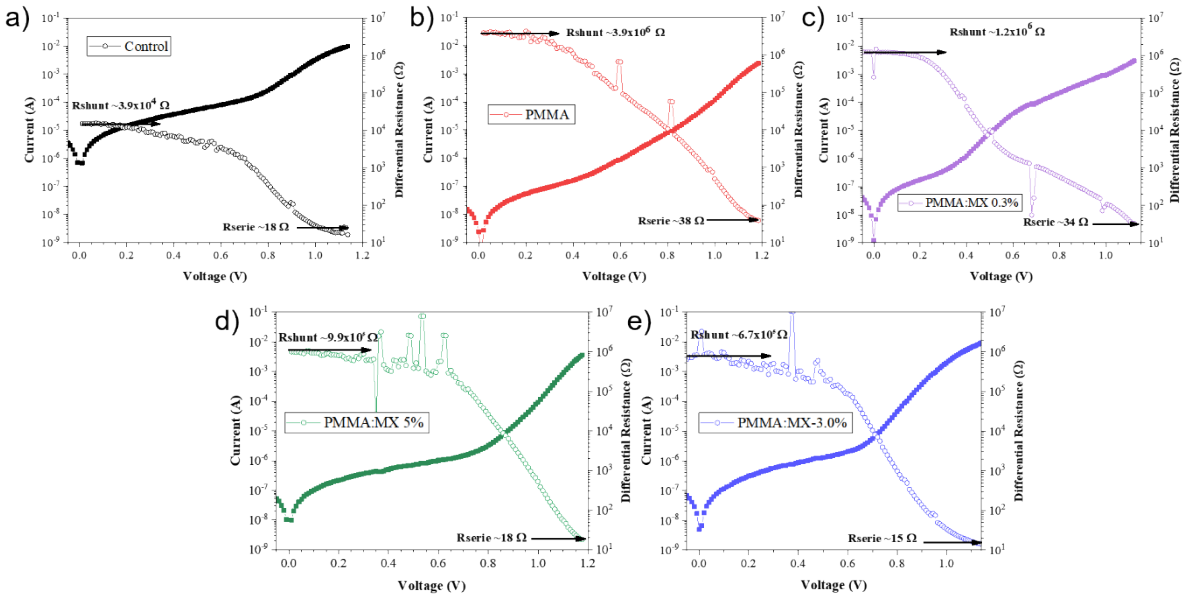

Figure S7: Current vs. voltage and differential resistance versus voltage curves of (a) Control, b) PMMA and (c-e) PMMA:MX (0.3, 1.5 and 3.0%) based devices, respectively.

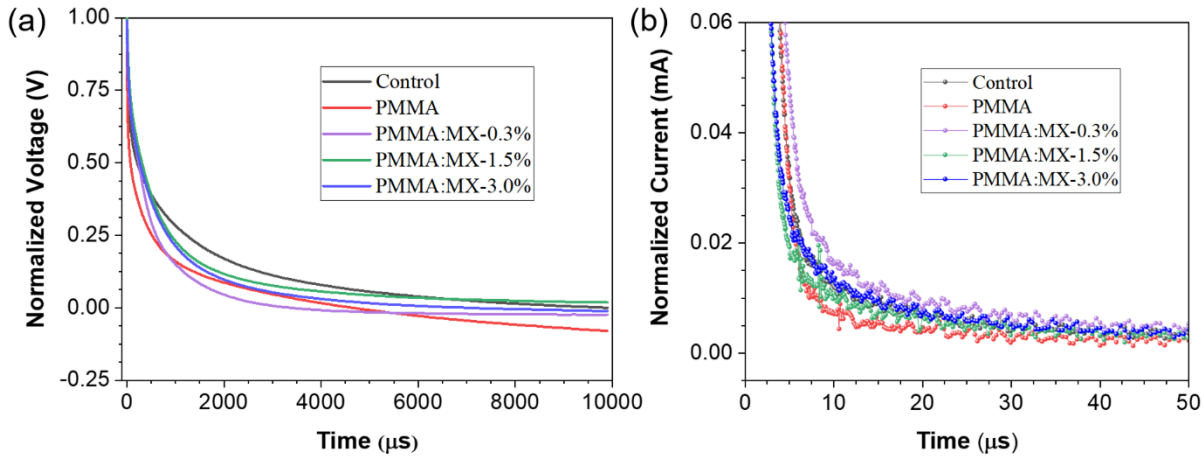

Figure S8: (a) TPV and (b) TPC curves of Control, PMMA and PMMA:MX based devices.

Table S2: Fitted parameters of the TPV and TPC curves of PSCs under 1 sun simulated irradiation (72 mW.cm^{-2}). The τ and t_e corresponds to the recombination and extraction charges obtained from TPV and TPC curves, respectively.

Device	A_1	τ_1 (µs)	A_2	τ_2 (ms)	τ (ms)	t_e(µs)
Control	0.37	26.3	0.75	0.88	0.88	1.47
PMMA	0.60	24.4	0.44	0.54	0.53	1.69
PMMA:MX-0.3%	0.45	24.2	0.63	0.67	0.67	1.59
PMMA:MX-1.5%	0.55	30.1	0.62	0.92	0.92	1.24
PMMA:MX-3.0%	0.45	28.7	0.71	0.80	0.80	1.16

The V_{OC} and TRPL decays were fitted using the following equation,

$$X(t) = A_1 \cdot exp\left(-\frac{t}{\tau_1}\right) + A_2 \cdot exp\left(-\frac{t}{\tau_2}\right) \quad \text{(Eq. S2)}$$

where A_1 and A_2 are constant, t is V_{OC} decay time, τ_1 and τ_2 are the fitted lifetimes.

The average lifetime, τ_x was calculated using the following equation:

$$\tau_x = \frac{A_1{\tau_1}^2 + A_2{\tau_2}^2}{A_1\tau_1 \cdot A_2\tau_2} \quad \text{(Eq. S3)}$$

The current decay was fitted using the following equation,

$$I(x) = A_1 \cdot exp\left(-\frac{x}{t_1}\right) \quad \text{(Eq. S4)}$$

where A_1 are constant, x is I decay time and $\mathbf{t_e}$ is the fitted charge extraction time.

Table S3: Fitted parameters of the TRPL of perovskite/PCBM, perovskite/PMMA/PCBM and perovskite/PMMA:MX/PCBM films.

Sample	A_1	τ_1 (ns)	A_2	τ_2 (ns)	τ_s (ns)
Control	41.51	111.20	57.49	2.06	108.47
PMMA	40.94	57.51	59.06	4.65	51.99
PMMA:MX-0.3%	23.76	53.71	76.24	4.13	43.90
PMMA:MX-1.5%	36.99	64.16	63.01	3.89	58.52
PMMA:MX-3.0%	38.49	82.50	61.51	3.17	77.91

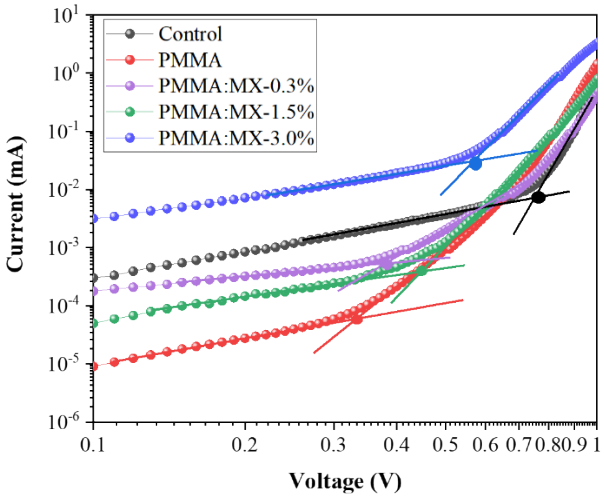

Figure S9: Dark I x V curves of Control, PMMA and PMMA:MX based devices showing respective V_{tfl}.

Estimation of the dielectric constant of the perovskite from the capacitance measurement of the device in the dark. Once the frequency choice at which to perform the Mott-Schottky analysis depends on the characteristics of the sample, we carried out the curves under 10, 55, and 100 kHz. We focused our analysis on the 100 kHz to overestimate the dielectric constant.

- $\varepsilon_0 = 8.85 \times 10^{-12}$ F m^{-1}

- d = 600 nm (PVK thickness)
- C_g = 3.26 x 10^{-4} F m^{-2}
  (from the control plot)
- ε = 21

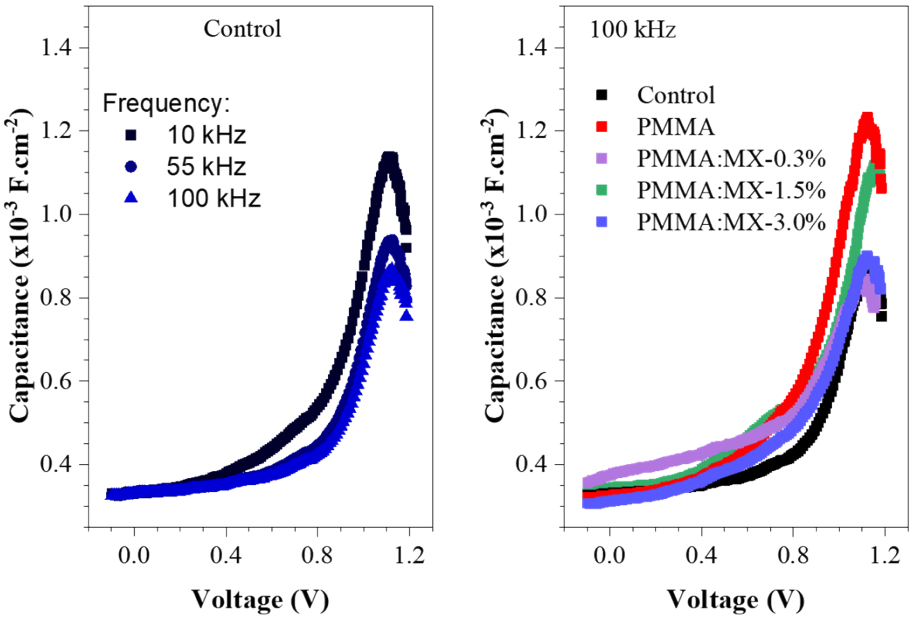

Figure S10: Capacitance-voltage curves carried out in the dark, at room temperature and under 50 mV of AC stimulus. a) Control device at 10, 55 and 100 kHz. b) Control, PMMA, PMMA:MX-1%, PMMA:MX-5% and PMMA:MX-10% devices at a fixed frequency of 100 kHz.

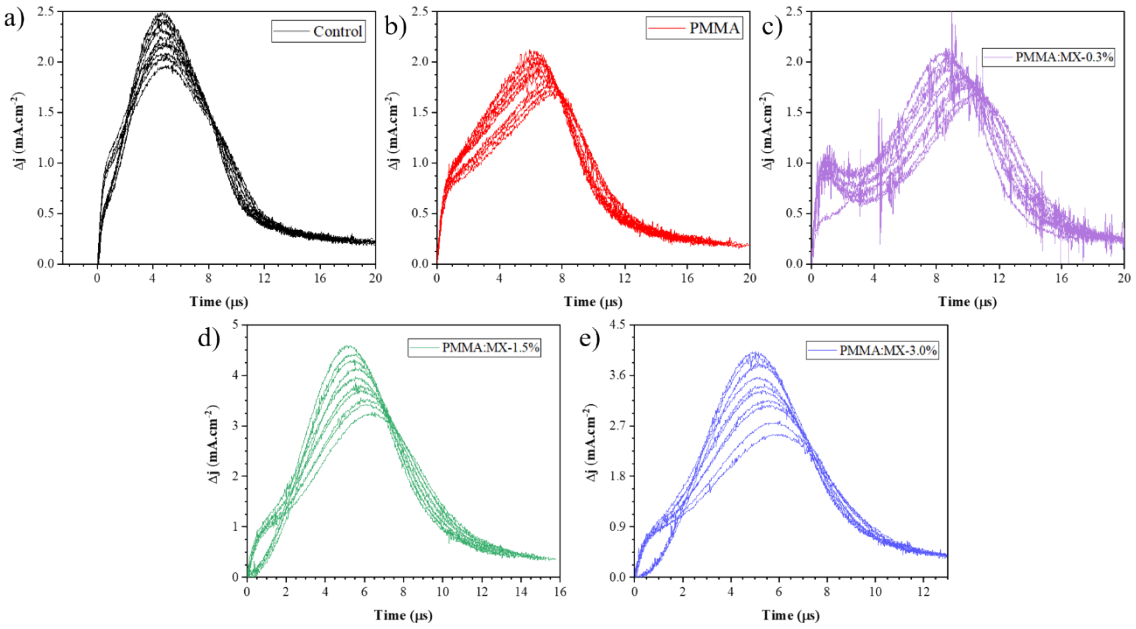

Figure S11: Δ*j* curves from Photo-CELIV measurements for Control, PMMA and PMMA:MX based PSCs.

Table S3: Devices' charge-transfer resistance (R_{ct}), recombination resistance (R_{rec}), built-in potential (V_{bi}) and capacitance at 1 HZ values (C_{1Hz}) of control, PMMA and PMMA:MX based PSCs.

Device	R_{ct} (kΩ)	R_{rec} (kΩ)	V_{bi} (V)	C_{1Hz} (μF)
Control	2.47	57.80	1.14	3.56
PMMA	2.22	39.45	1.09	5.86
PMMA:MX-0.3%	0.83	21.27	1.21	7.21
PMMA:MX-1.5%	1.99	50.23	1.21	1.72
PMMA:MX-3%	1.38	20.09	1.19	3.51

To calculate the $N_{t,IS}$ spectra (Fig. 12 - c) from Eq. 6, we took the derivative of the capacitance spectra (Fig. 12- b) and used the V_{bi} values extracted from Fig. 5.

The relation between the demarcation energy (E_ω) and the angular frequency of the applied AC signal (ω) is given by the following:

$$E_{\omega} = k_b T ln\left(\frac{\omega_0}{\omega}\right) \qquad \text{(Eq. S5)}$$

Where ω_0 is a temperature-independent coefficient termed the "attempt to escape frequency". The values of the density of traps taken from the low frequency are shown in the Table 2. According to Eq. S5, the quantized values are related to the deep-level defects.

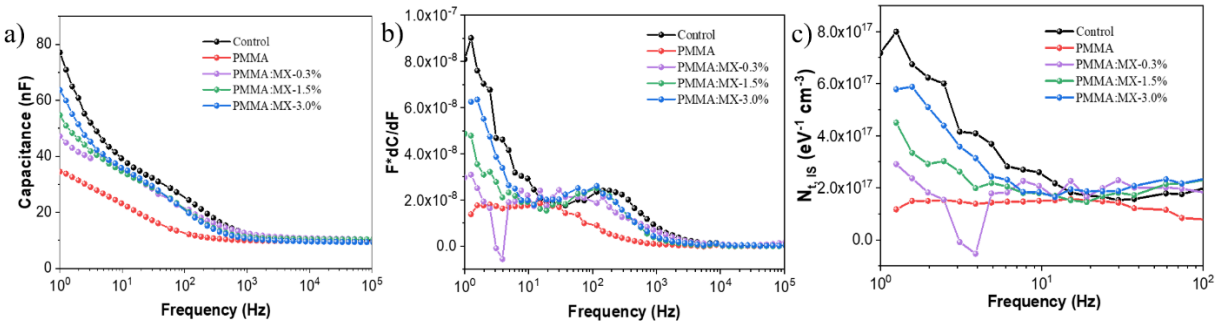

Figure S12: (a) Capacitance-frequency spectra and the (b) differential form of the spectra. (c) Defect density spectra at room temperature, in which the low-frequency values shown in the table are related to deep defect states. The measurements for the control, PMMA and PMMA:MX(0.3%, 1.5% and 3.0%) devices were performed under dark conditions and at zero bias voltage and an AC signal of 50 mV.